Supporting Information

Aqueous solution-processed off-stoichiometric Cu-In-S and their application in quantum dots-sensitized solar cell

Ya-Han Chiang,‡[a] Kuan-Yu Lin,‡[b] Yu-Hsuan Chen,[a] Keiko Waki,[c] Mulu Alemayehu Abate,[a] Jyh-Chiang Jiang,*[b] Jia-Yaw Chang*[a]

a. Nanochemistry Lab., Department of Chemical Engineering, National Taiwan University of Science and Technology, 43, Section 4, Keelung Road, Taipei, 10607, Taiwan, Republic of China

b. Computational and Theoretical Chemistry Lab., Department of Chemical Engineering, National Taiwan University of Science and Technology, 43, Section 4, Keelung Road, Taipei, 10607, Taiwan, Republic of China

c. Department of Chemical Science and Engineering, School of Materials and Chemical Technology, Tokyo Institute of Technology, 4259 Nagatsuta-cho, Midori-ku, Yokohama-shi 226-8502, Japan

‡ Ya-Han Chiang and Kuan-Yu Lin contributed equally to this work.

*Corresponding author: Jia-Yaw Chang, Jyh-Chiang Jiang

Department of Chemical Engineering, National Taiwan University of Science and Technology, 43, Section 4, Keelung Road, Taipei, 10607, Taiwan, Republic of China

E-mail: jychang@mail.ntust.edu.tw, jcjiang@mail.ntust.edu.tw

Tel.: +886-2-27303636.

Fax: +886-2-27376644.

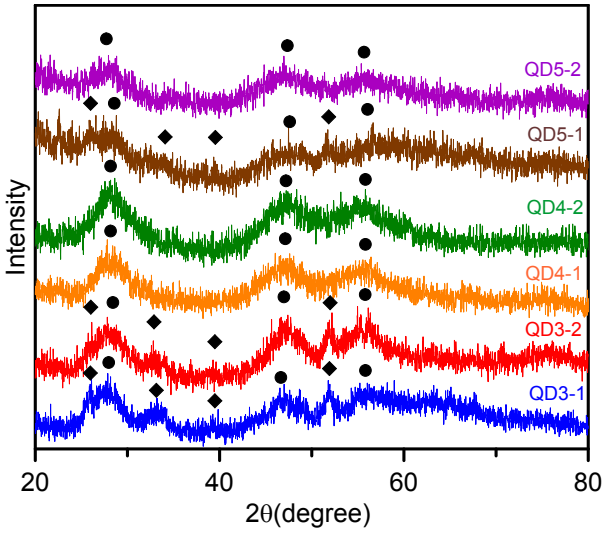

Figure S1. XRD patterns of different samples obtained at different molar ratios of the S/In precursors. The experiment conditions are summarized in Table S2. The diffraction peaks correspond to chalcopyrite $CuInS_2$ (JCPDS 75-0106, marked with ●) and cubic β-In_2S_3 (JCPDS 32-0456, marked with ◆).

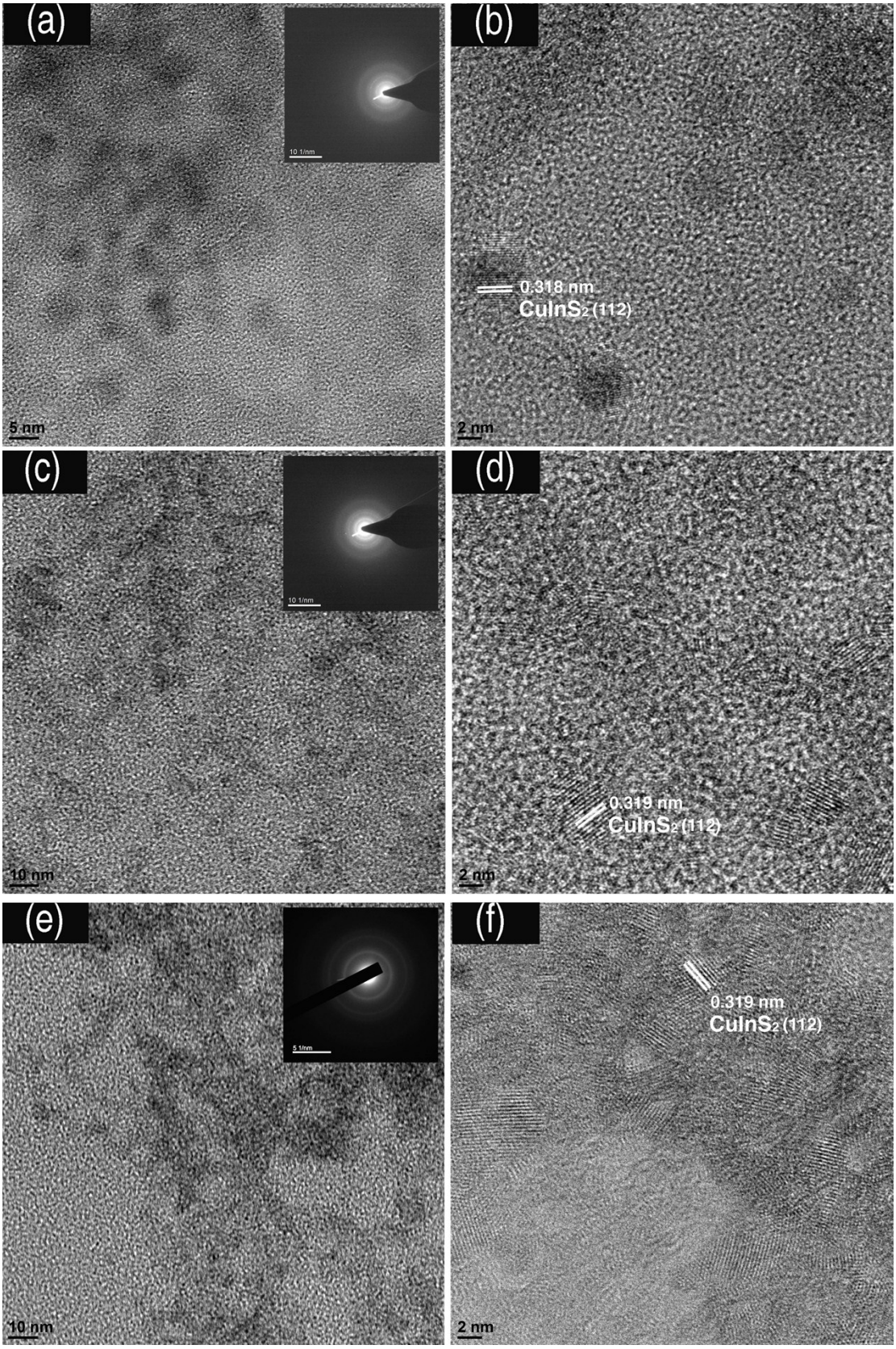

Figure S2. TEM (left panels) and high-resolution TEM (right panels) images of Samples (a, b) QD1, (c, d) QD2, and (e, f) QD3 prepared by various feed molar ratios of Cu : In. Inset: selected-area electron diffraction patterns of Samples QD1 (a), QD2

(c), and QD3 (e).

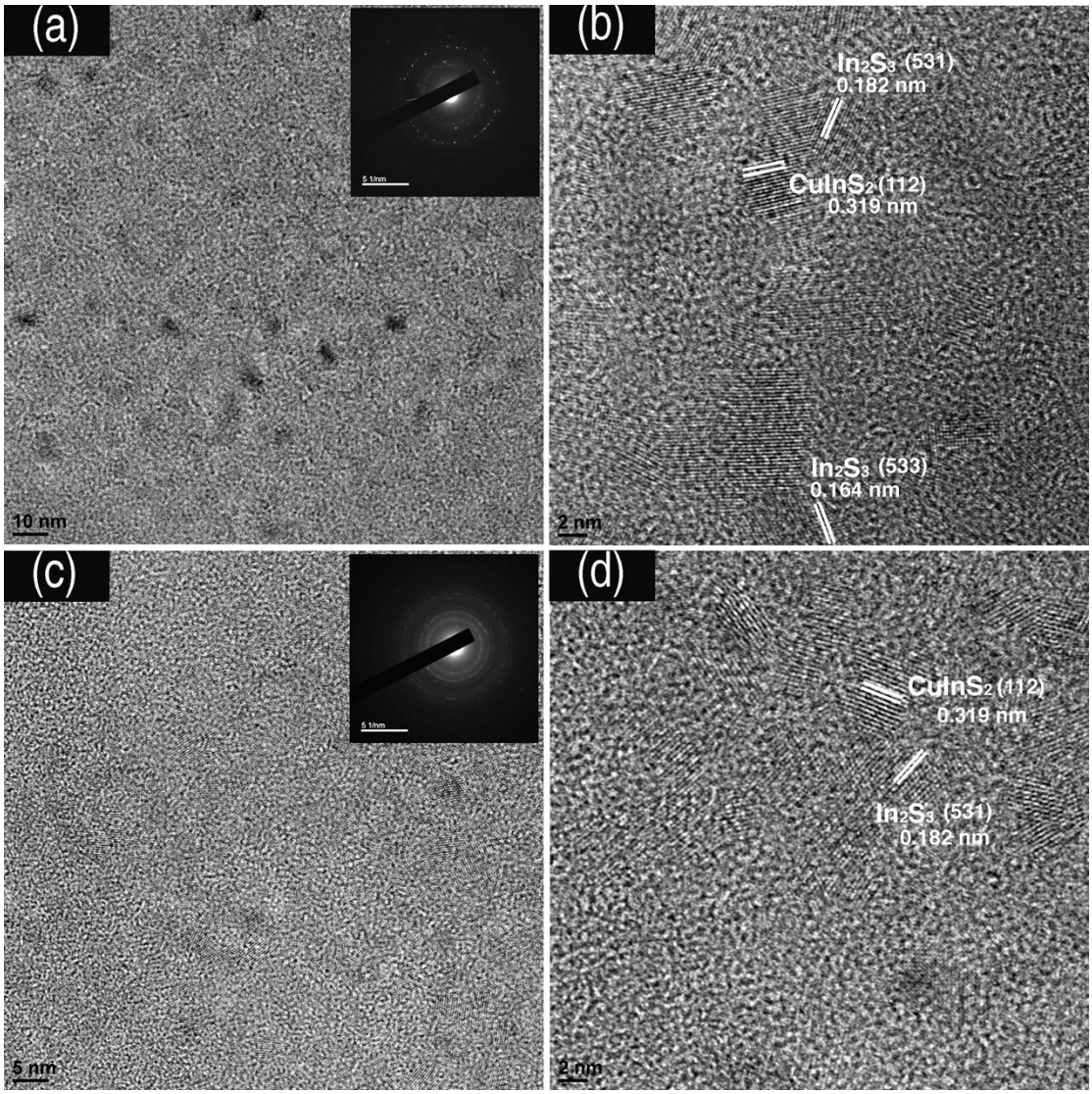

Figure S3. TEM (left panels) and high-resolution TEM (right panels) images of Samples (a, b) QD4 and (c, d) QD5 prepared by various feed molar ratios of Cu : In. Inset: selected-area electron diffraction patterns of Samples QD4 (a) and QD5 (c).

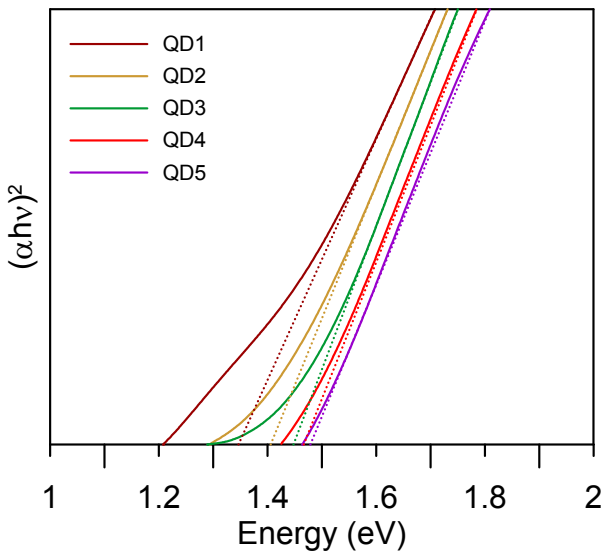

Figure S4. Plot of $(\alpha h\nu)^2$ versus energy for Samples QD1-QD5, where α represents the corresponding absorption and hν represents the photon energy.

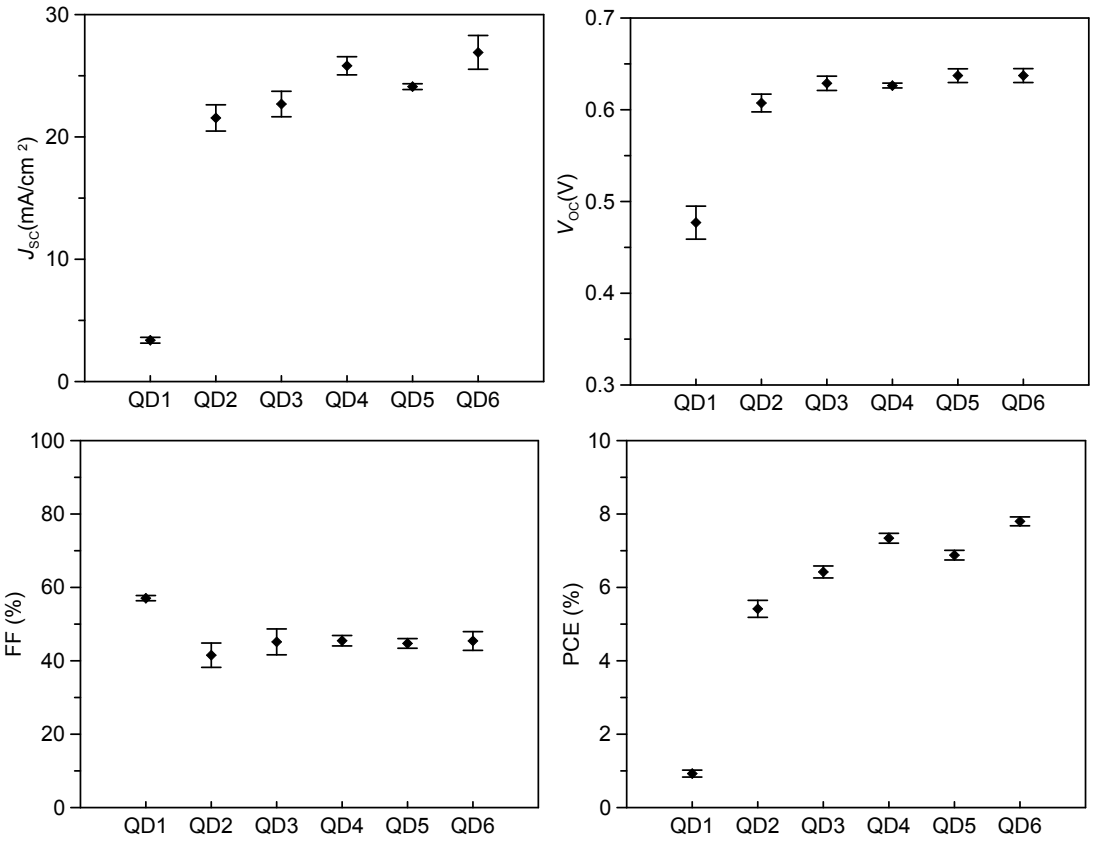

Figure S5. Summary of photovoltaic performance of Cells QD1-QD6. Error bars represent mean standard deviation of five independent experiments.

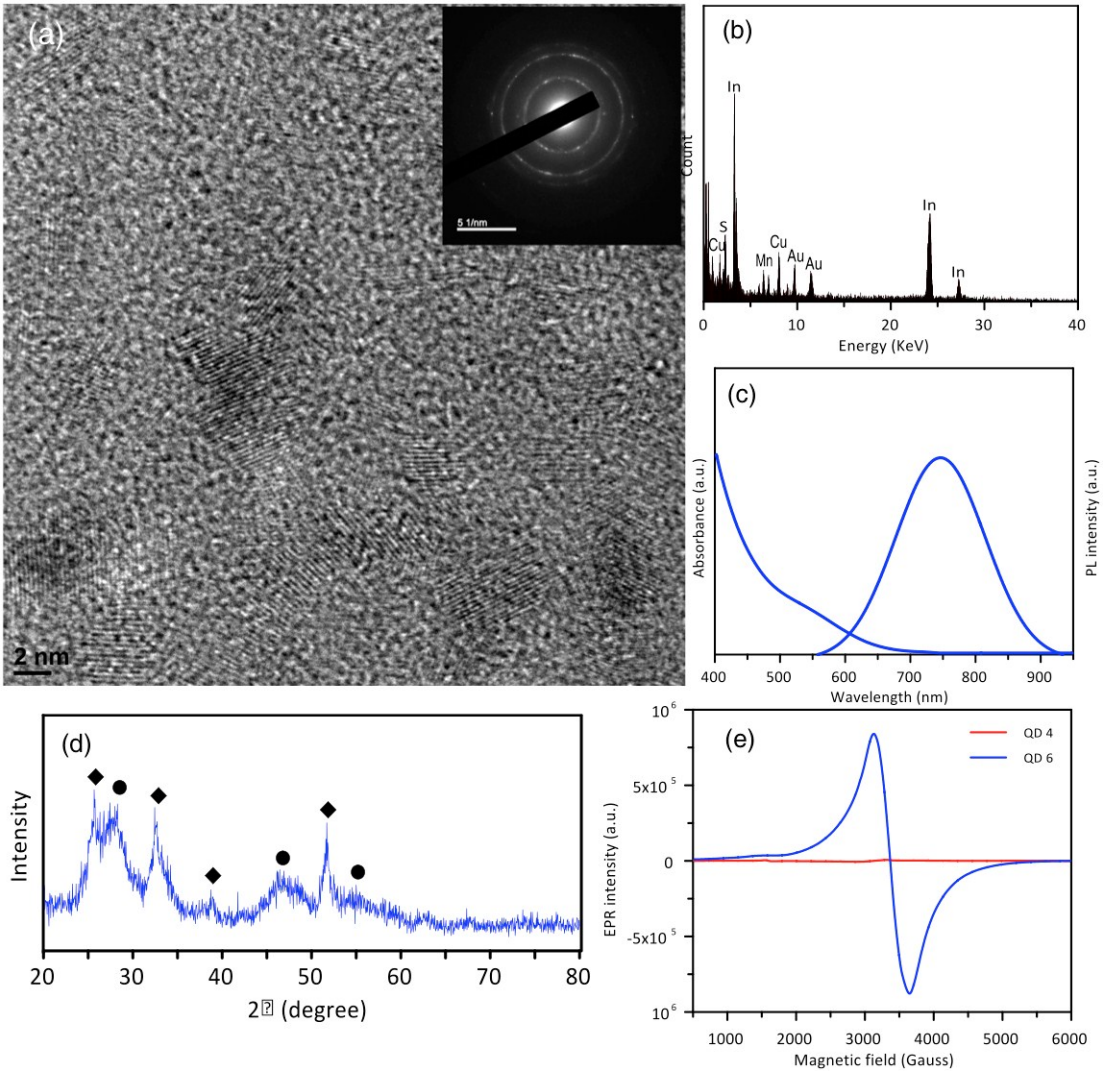

Figure S6. (a) High-resolution TEM images and (b) EDS spectrum of Samples QD6. The Au signals in the EDS measurement are from the gold grid. Inset: selected-area electron diffraction patterns of Samples QD6. (c) UV-vis absorption/photoluminescence spectra of Sample QD6. (d) XRD pattern of Sample QD6. The diffraction peaks show the chalcopyrite $CuInS_2$ (JCPDS 75-0106, marked with●) and cubic β-In_2S_3 (JCPDS 32-0456, marked with ◆). (e) EPR spectra obtained from Samples QD4 and QD6 measured at 10 K.

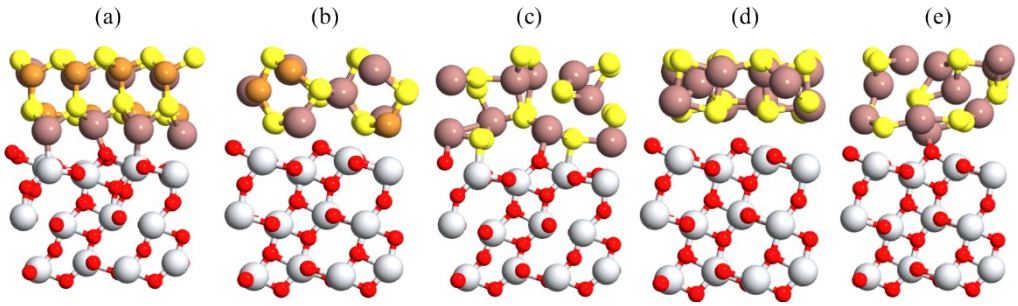

Figure S7. Calculation for the lowest-energy configurations of anatase TiO_2 (110) surface coated with (a) $CuInS_2$ (112) surface, (b) $CuInS_2$ (220) surface, (c) In_2S_3 (311) surface, (d) In_2S_3 (400) surface, and (e) In_2S_3 (440) surface. O atoms in red, Ti in white, S in yellow, In in brown, and Cu in gold.

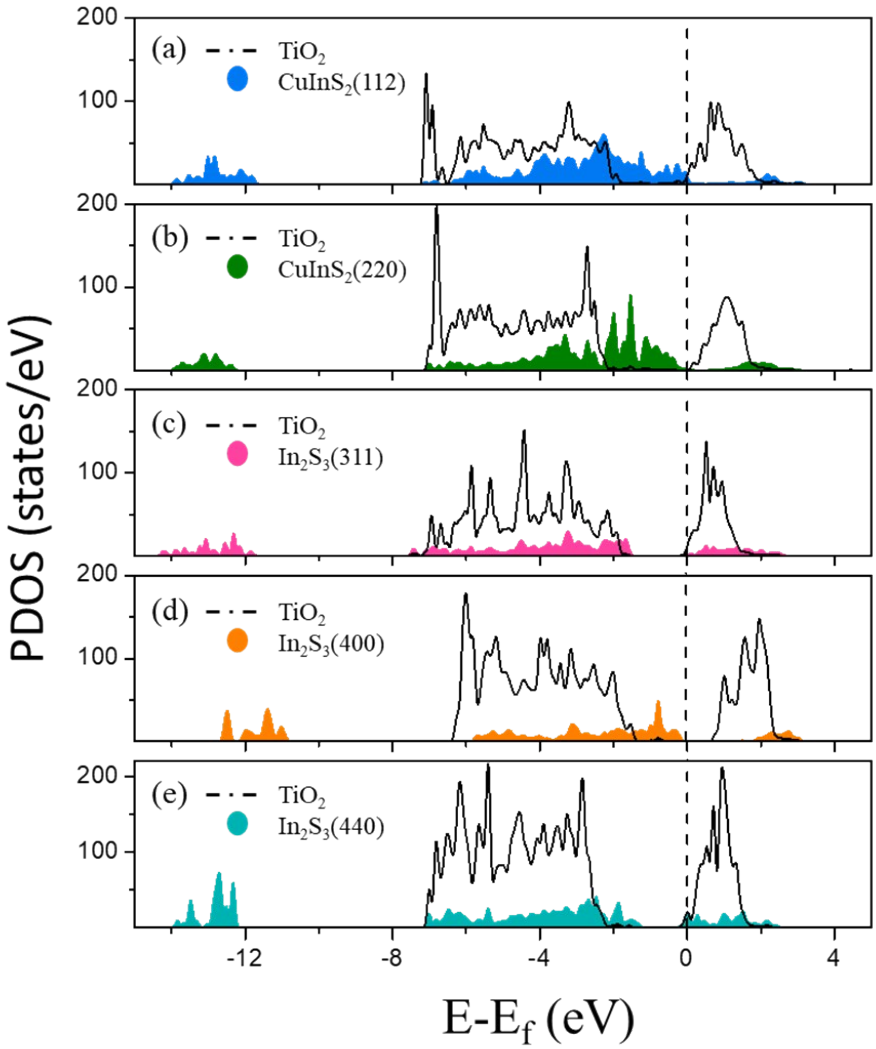

Figure S8. Calculation of project density of states (PDOS) for different QDs adsorbing on the anatase TiO_2 (110) surface: (a) $CuInS_2$ (112), (b) $CuInS_2$ (220), (c) In_2S_3 (311), (d) In_2S_3 (400), and (e) In_2S_3 (440). The black solid curves in (a)-(e): total DOS of TiO_2. The color-filled curves: adsorbate-projected DOS of coating QDs.

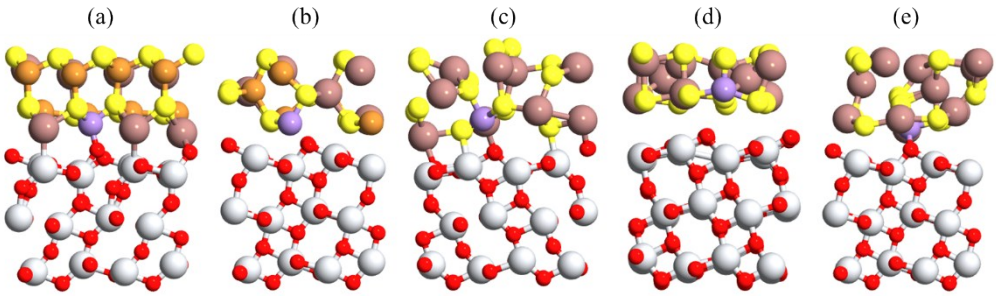

Figure S9. Calculation for the lowest-energy configurations of anatase TiO_2 (110) surface coated with Mn-doped QDs: (a) Mn:$CuInS_2$ (112) surface, (b) Mn:$CuInS_2$ (220) surface, (c) Mn:In_2S_3 (311) surface, (d) Mn:In_2S_3 (400) surface, and (e) Mn:In_2S_3 (440) surface. O atoms in red, Ti in white, S in yellow, In in brown, Cu in gold, and Mn in purple.

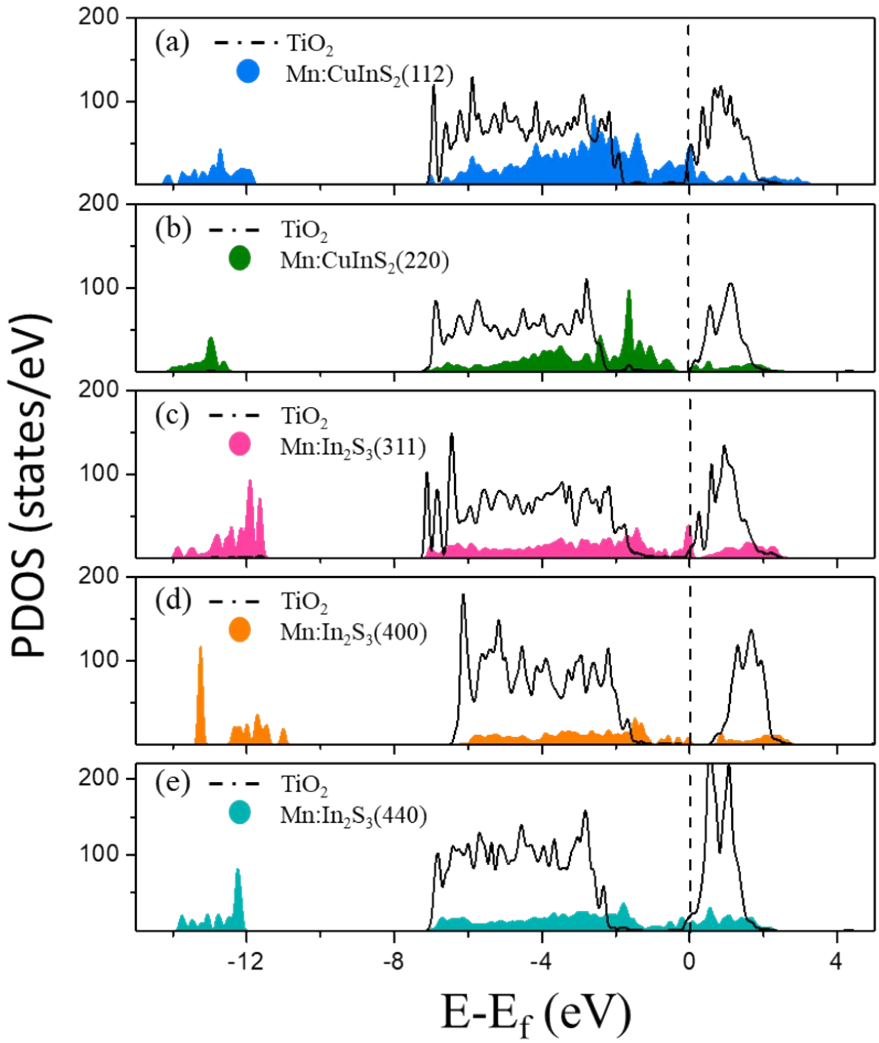

Figure S10. Calculation of project density of states (PDOS) for different Mn-doped QDs adsorbing on the anatase TiO_2 (110) surface: (a) Mn:$CuInS_2$ (112), (b) Mn:$CuInS_2$ (220), (c) Mn:In_2S_3 (311), (d) Mn:In_2S_3 (400), and (e) Mn:In_2S_3 (440). The black solid curves in (a)-(e): total DOS of TiO_2. The color-filled curves: adsorbate-projected DOS of coating QDs.

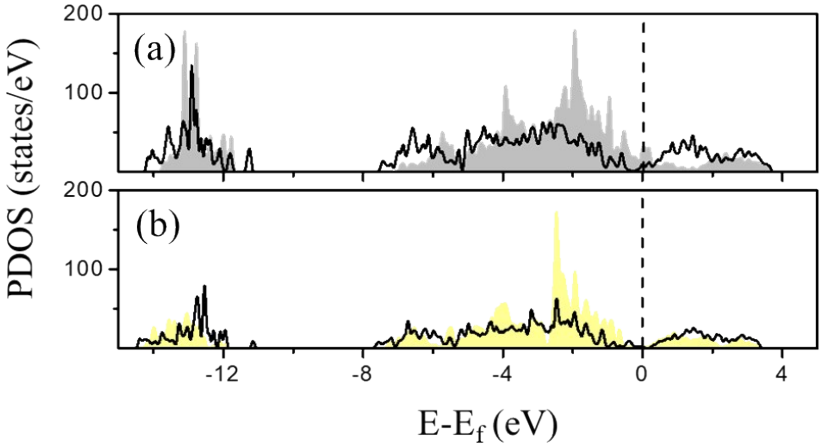

(c) $In_2S_3(311)/CuInS_2(112)$ (d) $In_2S_3(311)/CuInS_2(220)$

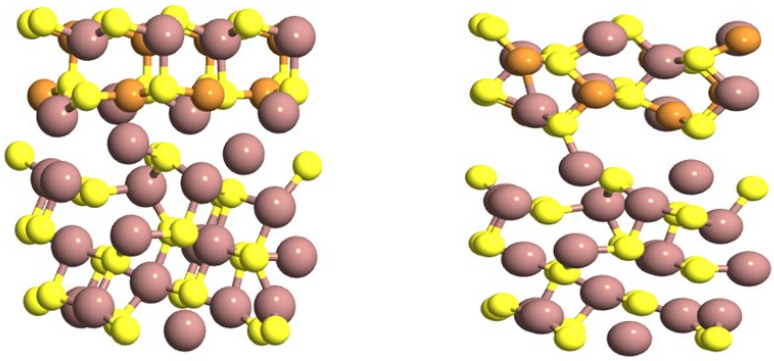

Figure S11. PDOS of (a) $In_2S_3(311)/CuInS_2(112)$ and (b) $In_2S_3(311)/CuInS_2(220)$. The black solid curves: total DOS of TiO_2. The color-filled curves: adsorbate-projected DOS of coating Mn-doped QDs. Optimized geometries for (c) $In_2S_3(311)/CuInS_2(112)$ and (d) $In_2S_3(311)/CuInS_2(220)$. O atoms in red, Ti in white, S in yellow, In in brown, and Cu in gold.

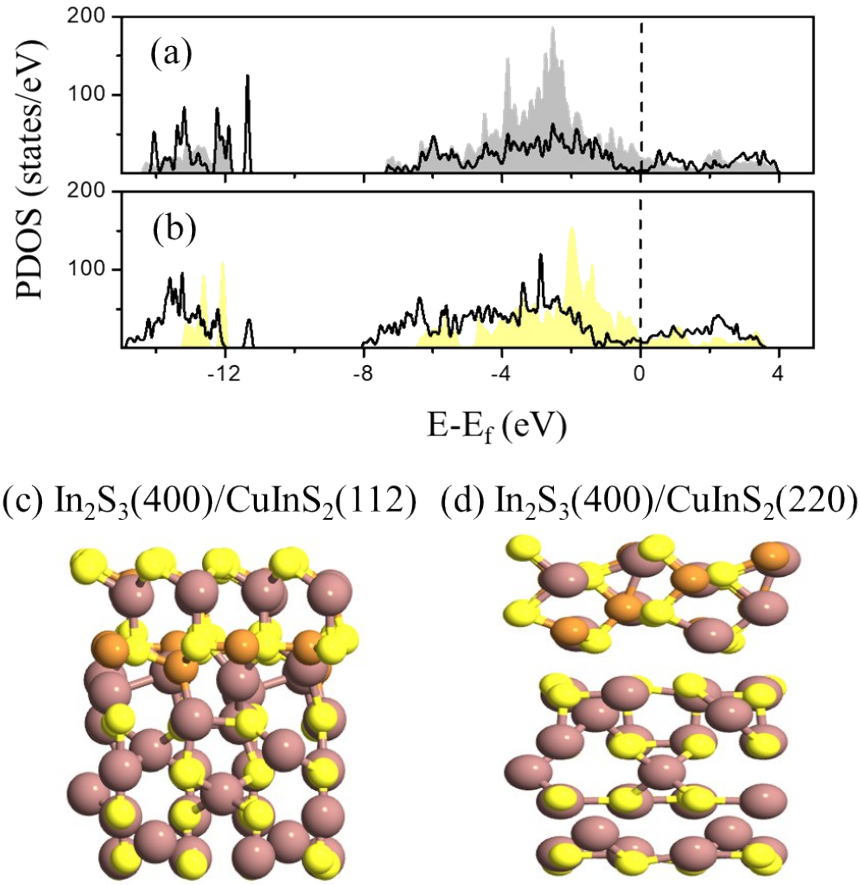

Figure S12. PDOS of (a) In_2S_3(400)/$CuInS_2$(112) and (b) In_2S_3(400)/$CuInS_2$(220). The black solid curves: total DOS of TiO_2. The color-filled curves: adsorbate-projected DOS of coating Mn-doped QDs. Optimized geometries for (c) In_2S_3(400)/$CuInS_2$(112) and (d) In_2S_3(400)/$CuInS_2$(220). O atoms in red, Ti in white, S in yellow, In in brown, and Cu in gold.

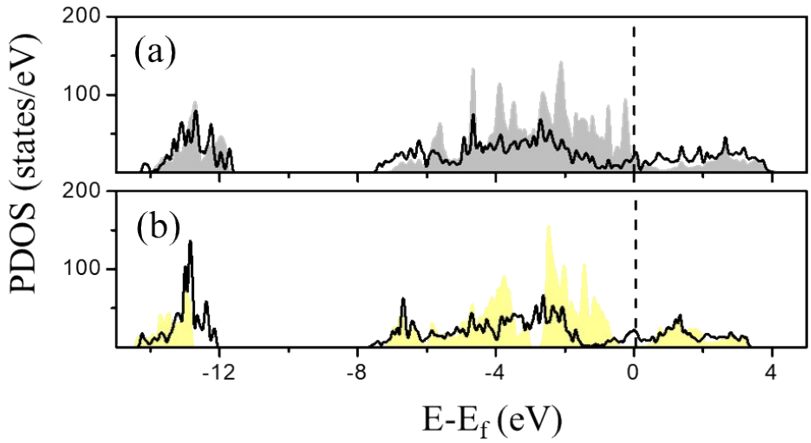

(c) In_2S_3(440)/$CuInS_2$(112) (d) In_2S_3(440)/$CuInS_2$(220)

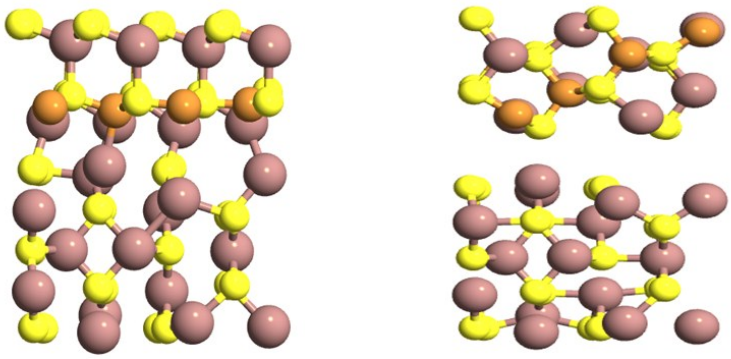

Figure S13. PDOS of (a) In_2S_3(440)/$CuInS_2$(112) and (b) In_2S_3(440)/$CuInS_2$(220). The black solid curves: total DOS of TiO_2. The color-filled curves: adsorbate-projected DOS of coating Mn-doped QDs. Optimized geometries for (c) In_2S_3(440)/$CuInS_2$(112) and (d) In_2S_3(440)/$CuInS_2$(220). O atoms in red, Ti in white, S in yellow, In in brown, and Cu in gold.

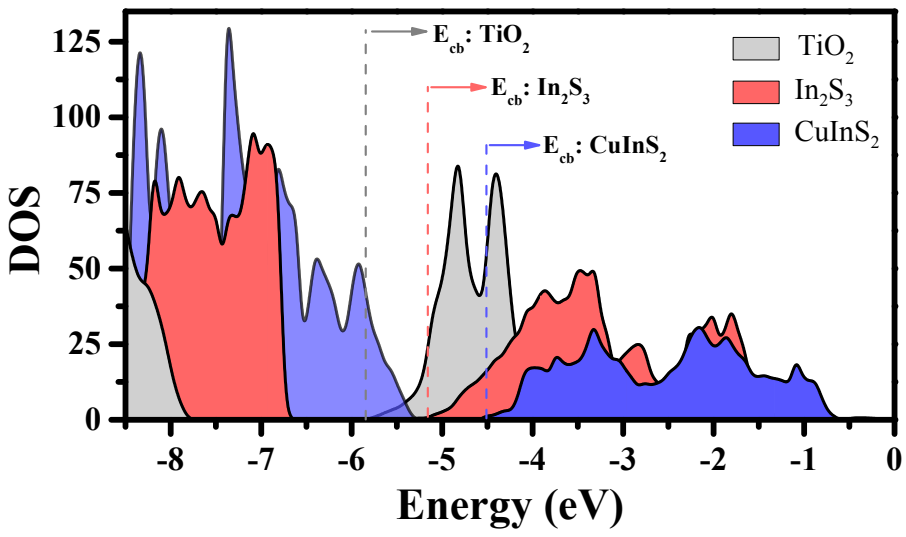

Figure S14. The total DOS calculation for the TiO_2, In_2S_3 and $CuInS_2$. (E_{cb} is referred to the conduction band edge and indicated by the dashed line.)

Table S1. Summary of different precursors used in the reaction for the preparation Samples QD1-QD6.

Sample NO.	Cu (mmol)	In (mmol)	Mn (mmol)	L-cysteine (mmol)	Na_2S (mmol)
QD1	1.25×10^{-2}	1.25×10^{-2}	-	8.8×10^{-2}	4.8×10^{-2}
QD2	1.25×10^{-2}	2.50×10^{-2}	-	8.8×10^{-2}	4.8×10^{-2}
QD3	1.25×10^{-2}	3.75×10^{-2}	-	8.8×10^{-2}	4.8×10^{-2}
QD4	1.25×10^{-2}	5.00×10^{-2}	-	8.8×10^{-2}	4.8×10^{-2}
QD5	1.25×10^{-2}	6.25×10^{-2}	-	8.8×10^{-2}	4.8×10^{-2}
QD6	1.25×10^{-2}	5.00×10^{-2}	1.25×10^{-3}	8.8×10^{-2}	4.8×10^{-2}

Table S2. Summary of different precursors used in the reaction for the control experiment

Sample NO.	Cu (mmol)	In (mmol)	L-cysteine (mmol)	Na_2S (mmol)	[S]/[In]
QD3-1	1.25×10^{-2}	3.75×10^{-2}	8.8×10^{-2}	2.88×10^{-2}	0.768
QD3-2	1.25×10^{-2}	3.75×10^{-2}	8.8×10^{-2}	3.6×10^{-2}	0.96
QD4-1	1.25×10^{-2}	5.00×10^{-2}	8.8×10^{-2}	6.4×10^{-2}	1.28
QD4-2	1.25×10^{-2}	5.00×10^{-2}	8.8×10^{-2}	9.6×10^{-2}	1.92
QD5-1	1.25×10^{-2}	6.25×10^{-2}	8.8×10^{-2}	8.0×10^{-2}	1.28
QD5-2	1.25×10^{-2}	6.25×10^{-2}	8.8×10^{-2}	12.0×10^{-2}	1.92

Table S3. Calculated adsorption energy (E_{ads}), the change of bader charges (ΔQ), and the percentage of conduction band overlap (%) for TiO_2 (110) surface with different QDs and Mn-doped QDs

Adsorption on TiO_2 (110)	E_{ads} (eV/ Å^2)	ΔQ (e) TiO_2/ QDs	Conduction Band Overlap (%)
$CuInS_2$ (112)	-0.19	-1.26	36.0
$CuInS_2$ (220)	-0.07	-0.48	66.5
In_2S_3 (311)	-0.32	-0.82	65.8
In_2S_3 (400)	-0.26	-0.12	68.2
In_2S_3 (440)	-0.18	-1.59	85.2
Mn:$CuInS_2$ (112)	-0.11	-1.29	65.1
Mn:$CuInS_2$ (220)	-0.14	-0.59	76.9
Mn:In_2S_3 (311)	-0.22	-0.85	78.0
Mn:In_2S_3 (400)	-0.18	-0.31	82.9
Mn:In_2S_3 (440)	-0.08	-1.62	95.3